The role of cellular contractility in topography sensing on soft nanoporous polyacrylamide hydrogels

Beatriz Rebollo Calderón

Jordi Comelles, Institute of Bioengineering of Catalonia (IBEC)

Abstract—**Extracellular matrix physical characteristics have been shown to play an important role in cellular processes such as adhesion, migration, proliferation and differentiation. Of high importance are the stiffness and the topography of the extracellular matrix, which are believed to activate shared signalling pathways to cause a cellular response. In this work, we use polyacrylamide nanoporous hydrogels of different stiffness, both with and without microtopographical structures to see if these physical cues are truly sensed by the same mechanism, and an inhibitor of ROCK I to determine the role of cell contractility in the sensing of topography and stiffness.**

2. Nanobiotecnology—**mechanosensing, hydrogels, synthetic extracellular matrix, surface topography.**

I. Introduction

Living cells interact with their surroundings, such as other cells and the extracellular matrix (ECM). They stablish a bidirectional communication to receive external inputs that can be integrated and generate a cellular response, and to send signals to other cells and the ECM, that can alter cell behaviour or ECM characteristics. ECM cues, both chemical and physical, can influence a wide range of cellular aspects, such as cell adhesion, shape, migration, proliferation and differentiation, by the activation of biologically preserved mechanisms [1].

The ECM is composed by a nanoporous network of diverse connective tissue components, and gives physical support to the cells, as well as regulating biochemical signalling. Cell-ECM interactions are governed by three main ECM characteristics: (i) stiffness, (ii) topography and (iii) ligand presentation [2]. ECM stiffness plays an important role in contractile-based mechanotransduction, which has been shown to affect the cell differentiation lineage [3]. ECM topography has been shown to cause contact guidance, a phenomenon that affects cell migration and morphology [4]. Moreover, it has been seen that in some types of breast and pancreas cancer there is a reorganization of the ECM collagen fibres that surround the
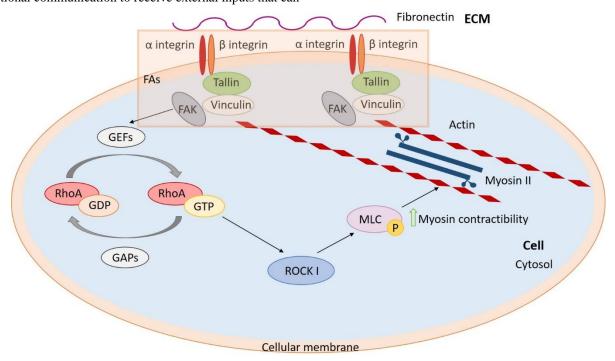

Fig. 1. Focal adhesion, actin cytoskeleton and intracellular signaling events involved in mechanosensing.

tumour. Cancer associated fibroblast cells reorganize the structure of the collagen into radial collagen fibres, pointing outwards the tumour. These fibres are then used as tracks through which cancer cells orient and migrate, thus increasing tissue invasion and metastasis. Scanning electron microscopy and second harmonic microscopy analysis show that those collagen tracks are composed by micrometric sized (1-2 μm in width) bundles of nanometric collagen fibres [5],[6]. Due to the critical role of metastasis in cancer progression, several works have addressed the question of how cells align and orient along the underlying matrix topography *in vitro*. These works found that cell alignment and migration can be guided by micro and nanostructures on topographically modified polymeric materials [6]. They also suggest that this is due to the confinement of cell-ECM adhesion sites produced by the substrate topography.

The most important of cell-ECM adhesion mechanisms is the integrin-mediated adhesion, which produces the so-called focal adhesion (FA) structures. FAs (*Fig. 1*) are physical and biochemical bridges that transduce mechanochemical signals from the ECM to the cell and *vice versa* [7],[8]. They are dynamic structures that form as nascent adhesions when integrins bind to their ECM ligands (mainly fibronectin, collagen and laminin proteins), and to actin, a protein of the cell cytoskeleton. Later, they progress to mature FA in a force-mediated manner. Nascent adhesions bound to the ECM exert a deformation on it, and a progressive force loading, which is higher for stiffer ECMs. At high forces, integrins form aggregations or clusters, and recruit intracellular proteins, culminating in the strengthening of the nascent adhesion to mature FA [9]. One of the main differences between nascent and mature FA is the presence of stress fibres. These are arrays of filaments that contain both actin and myosin II, which give them contractile activity. Therefore, FA fate is strongly dependent on both the stiffness of the underlying ECM and the contractile activity of the cell. Contractile activity is also key in processes such as cell spreading and migration [10].

Some cellular responses to the physical properties of the environment are due to changes in gene expression triggered by the activation of intracellular signalling pathways [7]. These pathways are thought to be initiated by a protein called focal adhesion kinase (FAK), which is one of the main regulatory elements of the mechanosensing activity of FA. FAK is a tyrosine kinase that can bind and activate several guanine-nucleotide exchange factors (GEFs) that promote the interchange of GDP to GTP in GTPases, thus activating them. These GEFs have been found to promote the activation of small Rho family GTPases. The main result of the activation of FAK is that, in turn, it activates RhoA, which enhances myosin II-dependent contractility through the downstream serine-threonine kinase ROCK [11]. ROCK phosphorylates the myosin light chain (MLC) and the MLC phosphatase, thus increasing the actin binding of myosin II [12]. This results in an overall increase of the contracile capacity of the cell, in other words, the capacity to exert a mechanical stress.

Of special interest is also the Yes-associated protein (YAP). As its intracellular location varies in different mechanical
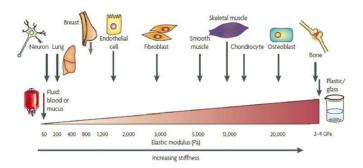

Fig. 2. ECM stiffness of tissues *in vivo* [1].

conditions, it is considered a sensor of mechanical cues, but not of topographical ones [13]. YAP is a transcriptional co-factor that translocates into the cell nucleus, and this leads to processes related to cell proliferation, cell survival, cell differentiation, tissue regeneration and organ size [14]. YAP localization is controlled by the stiffness of the ECM or the cell culture substrate: cells cultured on hard substrates show non-phosphorylated YAP, which can translocate to the nucleus and lead to changes in the genetic expression of the cell, whereas cells cultured in softer substrates present phosphorylated YAP, which remains in the cytosol, where it is degraded.

It has been theorised that cells use the same mechanism to respond to both substrate stiffness and topography. However, reported experiments dealing with substrate topography sensing are performed using substrates of high stiffness which are not physiologically relevant, as stiffness of biological tissues ranges between 50 Pa in liquid tissues such as blood, to 2 GPa in bone (*Fig. 2*) [1]. For example, some of the materials that have been used are Ti_6Al_4V [15], quartz [16], PDMS [17] and cyclic olefin copolymer [18], which correspond to stiffness of: 110 GPa, 76.5 GPa, 0.8-1.6 GPa and 1.5-2.2 GPa, respectively, all stiffness way above the physiological range. So, there is the need for experiments performed on experimental set-ups that include topography on soft substrates, which represent better the physiological conditions, and that allow us to explore the role of topography and stiffness, in a disentangled manner. In addition, they will allow us to assess the role of cell contractility in relation to the sensing of topography. In this work, we use polyacrylamide (PAA) nanoporous hydrogels with topographical microstructures and three different stiffness, with and without inhibiting cell contractility to study the effects of these three parameters in cell morphology. As topography, we selected 2 μm wide lines, which mimic the structures reported to be relevant for cancer metastasis *in vivo* [6]. To prevent cell contractility, we use Y-27632 chemical to inhibit ROCK and affect cell cytoskeleton. We first fabricated the hydrogels and characterized them by optical microscopy, scanning electron microscopy and atomic force microscopy. Then, we studied the effect of stiffness, topography and contractility in cell morphology. Finally, we explored the activation of mechanosensing pathways due to those cues by determining the cellular localization of YAP. Our results aim to contribute in assessing if cellular contractility is involved in the cell sensing

TABLE I
POLYACRYLAMIDE HYDROGEL COMPOSITION

Stiffness	Reagent	Percentage (v/v)
Stock solution		
Soft	Acrylamide (40%)	75%
	Bis-acrylamide (2%)	15%
	H_2O	10%
Medium	Acrylamide (40%)	60%
	Bis-acrylamide (2%)	15%
	H_2O	25%
Hard	Acrylamide (40%)	45%
	Bis-acrylamide (2%)	45%
	H_2O	10%
Working solution		
Soft	Stock solution	25%
	H_2O	74.35%
	Ammonium persulfate	0.5%
	N,N,N',N'-tetramethylethylenediamine	0.15%
Medium	Stock solution	50%
	H_2O	49.35%
	Ammonium persulfate	0.5%
	N,N,N',N'-tetramethylethylenediamine	0.15%
Hard	Stock solution	64.75%
	H_2O	34.6%
	Ammonium persulfate	0.5%
	N,N,N',N'-tetramethylethylenediamine	0.15%

of the substrate stiffness and/or topography.

II. METHODS

A. Preparation of polyacrylamide (PAA) hydrogels

PAA hydrogels with both topography and flat surfaces (which served as control) were produced following a modified version of a protocol described elsewhere [19]. Hydrogels of different stiffness (termed soft, medium and hard) were fabricated by mixing different percentages of acrylamide (BioRad) and bis-acrylamide (Sigma-Aldrich) (Table I); 0.5% (v/v) ammonium persulfate (Serva) and 0.15% (v/v) N,N,N',N'-tetramethylethylenediamine (Sigma-Aldrich) were used as initiators of the polymerization reaction. *Fig. 3* shows the schematic fabrication process of these hydrogels with topography. First, a polydimethylsiloxane (PDMS) mold was fabricated by spinning PDMS upon a silicon wafer with the topography at 500 rpm for 10 seconds and at 1000 rpm for 30 seconds using a Spin coater WS-650MZ-23NPP/LITE (Laurell Technologies Corporation). Then, the PDMS was cured in an oven at 65ºC overnight. Afterwards, the polyacrylamide solutions were placed between the PDMS mold and a glass coverslip and were let polymerize. The coverslips were previously activated by silanization to ensure the adherence of

the hydrogel to the glass. Before the silanization, the coverslips were cleaned by several sonication steps in different solutions: water with soap, water, distilled water, a solution of EDTA 1 mM (Sigma-Aldrich), 70% EtOH and 96% EtOH for 30 minutes each and afterwards, they were stored in 96% EtOH. Silanization was performed by incubating the coverslips in a shaker with 50% 3-aminopropyltrimethoxysilane (Sigma-Aldrich) for 5 minutes, then with water for 30 minutes, and finally with 0.5% glutardialdehyde (Sigma-Aldrich) for 30 minutes. Finally, coverslips were dried with N_2 and degassed. After PAA polymerization (typically 3 hours), the hydrogels were demoulded and bright field microscopy (Nikon Eclipse Ts2) was used to assess that the topography was present in the hydrogels. Finally, hydrogels were kept in distilled water between 24 and 48 hours to achieve equilibrium swelling.

B. SEM imaging

Scanning electron microscopy (SEM) was employed to check the morphology of the porous nature of the hydrogel samples and the structures created by the microfabrication process. Samples needed to be dried for imaging, and this was achieved by freeze-drying of the samples in liquid nitrogen followed by lyophilisation under vacuum. Then samples were imaged by a Nova NanoSEM 230 microscope (FEI company), using the low vacuum mode (0.5 mbar of water pressure) and low vacuum detector. These conditions allow the visualization of non-conductive samples, such as PAA without requiring coating with conductive materials.

C. Stiffness characterization by AFM

AFM (JPK Nanowizard 4) was used to assess the Young's modulus (E) of the hydrogels used in this work. First, the sensitivity was calibrated by performing a force-displacement curve on a hard surface (typically the coverslip region next to the hydrogel) prior to any measurement. Then, series of force-displacement (F-z) curves were measured on several points of the hydrogels (a minimum of 7 curves were performed on each sample) using a quadratic pyramidal tip with sides of 35° (Ө) and a nominal spring constant (k) of 0.08 N/m for the soft and medium stiffness hydrogels, and 0.32 N/m for the hard one. The Poisson's ratio (ν) of PAA used during data processing is 0.457 [20]. The force (F) on the cantilever was computed using the Hook's Law:

$$F = k \cdot d \qquad (1)$$

To compute E, force-displacement curves were analysed following the Hertz model of contact mechanics, which assumes the sample to be an isotropic and linear elastic solid and that there are not additional interactions between the tip and
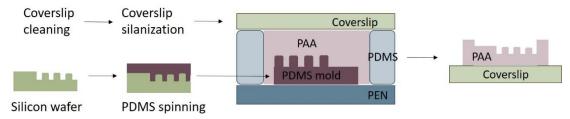

Fig. 3. Fabrication process of the PAA hydrogels

the sample. Therefore, F, E, ν and, δ (indentation depth) can be related by the following equation [21]:

$$F = \frac{E \tan\theta}{4(1-\nu^2)} \cdot \delta^2 \qquad (2)$$

D. PAA hydrogel functionalization

In order to improve cell adhesion on PAA hydrogels they were functionalized with ECM proteins. Among the different adhesion proteins present in the ECM, we selected fibronectin to promote a FA mediated adhesion. To covalently attach fibronectin to PAA we used Sulfo-SANPAH chemical reagent (3.8 mM) as a cross-linker. After the swelling, hydrogels were dried and Sulfo-SANPAH (Thermo Scientific) was added to the surface of the hydrogel and activated using UV light (Light Source LQ-HXP 120 UV) for 30 seconds [22]. Then, the excess of crosslinker was discarded by washing with water. Approximately, 20 µl of fibronectin from bovine plasma (Sigma-Aldrich) at a concentration of 20 µg/ml was added to each hydrogel, and then hydrogels were left at room temperature for an hour.

E. Cell seeding and culture

The NIH 3T3 mouse embryonic fibroblast cell line was grown for 3 days at 37ºC and 5% CO_2 in DMEM medium (Life Technologies) supplemented with 10% fetal bovine serum (FBS) and 1% Penicillin/Streptomycin. Prior to experiments, cells were trypsinized and re-plated on the hydrogels. To check the effects of cell contractility, Y-27632 (Sigma-Aldrich) at 20 µM (which is a ROCK I inhibitor) was added to some of the samples after three hours of seeding, whereas the others were kept as controls. Cells were incubated 24 hours at 37ºC and 5% CO_2. Then, cells were imaged by phase contrast (Nikon Eclipse Ts2) and processed for immunostaining.

F. Immunostaining

For the immunostaining cells need to be previously fixed. For this, the medium is washed with PBS (Life Technologies) three times, a solution of 10% formalin (Sigma-Aldrich) is added, and cells are left 30 minutes at room temperature. Afterwards, three more washes with PBS are done. Then, cell membranes need to be permeabilized to allow the antibodies entering the cell. This is done by incubating for 30 minutes with 0,2% (v/v) TritonX (Sigma-Aldrich). The next step is the blocking step of reactive sites, to eliminate any possible non-specific interactions of the antibodies with non-protein elements. For this, cells are incubated with a blocking solution containing 1% (v/v) BSA (Sigma-Aldrich), 3% (v/v) donkey serum (Millipore) and 0.2% (v/v) TritonX in PBS for 1-2 hours at room temperature on an orbital shaker. Then, the primary antibody can be added, diluted in a working buffer of 0.1% (v/v) BSA, 0.3% (v/v) donkey serum and 0.2% (v/v) TritonX in PBS and kept 1 hour at room temperature and then at 4ºC overnight. Next day, the secondary antibody can be added after three washes
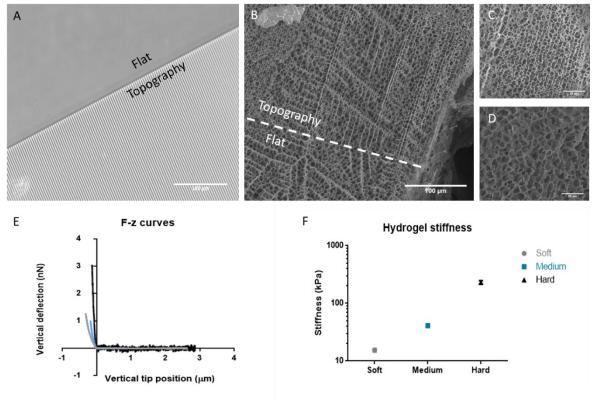

Fig. 4 A) Optical microscopy image of the boundary between the flat and topography areas of the 230.3 kPa hydrogel. Scale bar 100 µm. B) SEM image of the 15.4 kPa hydrogel. The dashed line marks the boundary between the flat area and the topography. Scale bar 100 µm. C) Magnification of the topography in B. Scale bar 20 µm. D) Magnification of the flat area in B. Scale bar 20 µm. E) Force-displacement curves measured by AFM on the soft, medium and hard hydrogels. F) Plot of the mean stiffness values: 15.4 kPa for the soft hydrogel, 41.1 kPa for the medium one and 230.3 kPa for the hard one.

with PBS. The secondary antibody is diluted in the same working solution previously described but without TritonX, and is left for at least an hour at room temperature. This secondary antibody contains the fluorescent molecule, so in the next steps the hydrogels need to be kept protected from the light. Finally, three more washes with PBS are done and DAPI (Sigma Aldrich) in a dilution 1:5000 is added in the working solution without TritonX is used to label the cell nuclei. The gels are mounted upside down on coverslips using Fluoromount-G (Sigma-Aldrich) and the samples are ready to be observed by fluorescence microscopy (Nikon Eclipse Ts2).

In this work, the antibodies used were mouse anti-YAP (Santa Cruz Biotechnology) at a1:250 dilution and anti – mouse 488 (Santa Cruz Biotechnology) at a 1:500 dilution. For staining of actin, Phalloidin-Rhodamine (Sigma-Aldrich) at a 1:40 dilution was also added together with the secondary antibody.

G. Data processing and statistics

ImageJ [23] was used to process the images obtained from bright field microscopy and fluorescence microscopy to gather information about both cell morphology and intracellular

localization of YAP, respectively. Cell morphology data obtained consisted on cellular area, cell alignment with respect to the topography lines, and cell elongation. Cell alignment is defined by using $\cos 2\Theta$ as a parameter, being Θ the angle between the major axis of the cells and the topography lines of the hydrogel. To compute cell elongation (E), cells are fitted by an ellipse, and its major (MA) and minor axis (ma) are determined. Elongation is then computed as:

$$E = \frac{MA - ma}{MA + ma} \tag{3}$$

.

This gives a value between 0 (round cells) and 1 (elongated cells). Intracellular localization of YAP was calculated by the ratio between the nucleus signal density and the cytoplasmatic signal density (N_{YAP}/C_{YAP}). AFM force curves were processed using JPK data processing software to obtain the stiffness values.
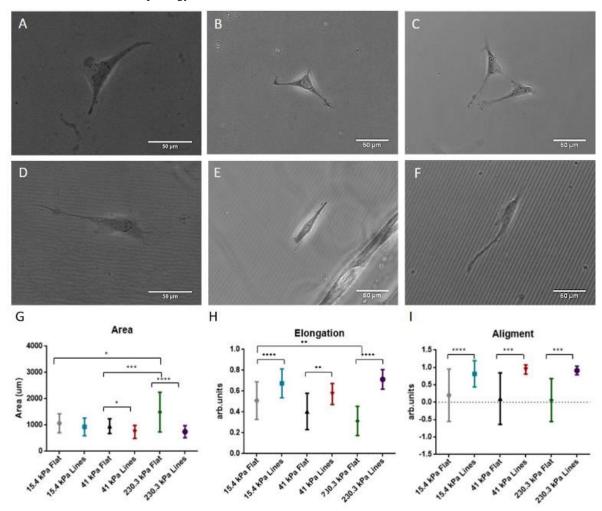

Fig. 5 Optical microscopy images of cells seeded on flat (A, B and C) and topographically modified (D, E and F) substrates on soft hydrogels (A and D), medium hydrogels (B and E) and hard hydrogels (C and F). Scale bar 50 μm. G) Quantification of the cellular area. H) Quantification of cellular elongation. I) Quantification of cellular alignment to topography lines.

H. Statistical analysis

All statistical analysis has been done with the One-way Anova test (*P<0.05, **P<0.01, ***P<0.001, ****P<0.0001). For the morphology study, a minimum of 2 independent experiments were done of each condition and a minimum of 8 cells were analyzed for each condition. In the case of the YAP localization experiments, a minimum of 2 independent experiments were done in the case of the soft and hard hydrogels and one experiment was done for the medium stiffness hydrogel. A minimum of 7 cells were analyzed for each condition.

III. RESULTS

A. Hydrogel nanoscale characterization

First, an optical characterization of the surface of the hydrogel was done to assess that the topography was present in the samples (Fig. 4 A). Then, SEM was used to study the surface at the nanoscale. In Fig. 4 B we can see the boundary between the lines of the topography and the flat surface. Fig. 4 C and D are magnifications of these two zones and the structural difference is evident. However, the size of the pores in Fig. 4 B, C and D is much bigger than expected, in the scale of micrometres instead of nanometres. Nevertheless, when comparing with other results obtained using the same sample preparation and imaging methodology [24], we can also see pores in the
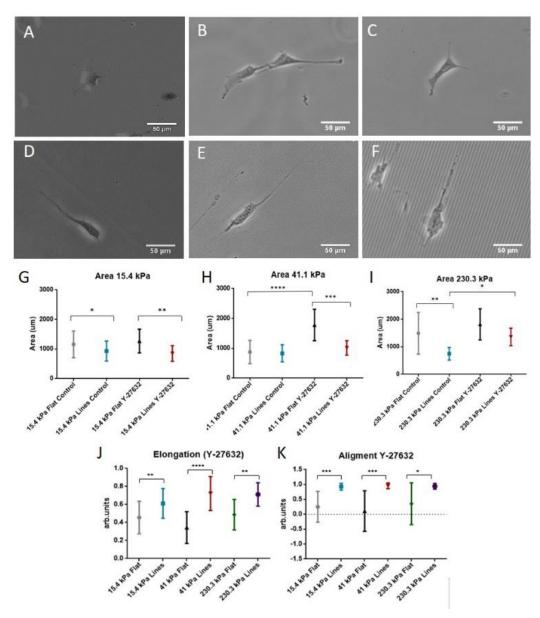

Fig. 6 Optical microscopy images of cells seeded on flat (A, B and C) and topographically modified (D, E and F) substrates without and with Y-27632 (20 µM) treatment. Images correspond to soft hydrogels (A and D), medium hydrogels (B and E) and hard hydrogels (C and F). Scale bar 50 µm. Quantification of the cellular area on flat and topographically modified substrates without (control) and with Y-27632 (20 µM) treatment on soft (G), medium (H) and hard hydrogels (I). J) Quantification of cellular elongation in presence of Y-27632 (20 µM).(K) Quantification of cellular alignment to topography in presence of Y-27632 (20 µM).

micrometre range (7.3±0.2 μm), similar to those in our samples (5.0±0.2 μm). Previous surface imaging by AFM performed by other groups members did not reveal this type of pores, so this porosity is probably a consequence of the lyophilisation process, which may have caused structural alterations in the polymer.

AFM was used to measure the stiffness of the PAA hydrogels. The stiffness values were obtained from fitting a Hertz model (*equation 2*) to the force-distance curves (*Fig. 4 E*). We obtained a Young's modulus of 15.4±0.4 kPa for the soft hydrogels, 41.1±0.7 kPa for the medium hydrogels and 230.3±4.9 kPa for the hard hydrogels (*Fig,4 F*). Although these values differ from those of reference [19], we successfully achieved our objective of obtaining three hydrogels of very different mechanical properties all laying within the ECM physiological range, which are suitable for the study of the role of cell contractility in topography sensing.

B. Cell morphology response to substrate stiffness and topography

In order to determine the role of cell contractility in topography sensing, we will first start by determining the response of contractile fibroblasts (without any treatment) to the topographical patterns of substrates with different stiffness. *Fig. 5 A-C* shows representative optical microscopy images of cells seeded in flat and *Fig. 5 D-F* show cells seeded on top of the topography. In the case of the cellular area, in *Fig. 5 G* we can see that there is a significant increase between the flat conditions of the soft and medium hydrogels compared to the hard hydrogel, so cellular area increases as stiffness increases in flat hydrogels. However, this effect is not seen in the presence of topography. On the contrary, cellular area shows a tendency to decrease as stiffness increases when cells are seeded on top of topography. Regarding the cellular elongation, cells tend to be rounder in flat than in topography samples. Moreover, as stiffness increases, cells become rounder in flat surfaces, whereas cell elongation in the presence of topography is not affected by the increase of stiffness (*Fig. 5 H*). Finally, cells seeded in flat have a random orientation, but in the case of cells seeded in topography this orientation is clearly aligned with the lines of the topography, and this effect is the same for all stiffness values (*Fig. 5 I*). Therefore, cells on flat surfaces increase their spreading area and circularity as stiffness increases, whereas cells on topography spread less, elongate and align with the topographical pattern in a stiffness independent manner.
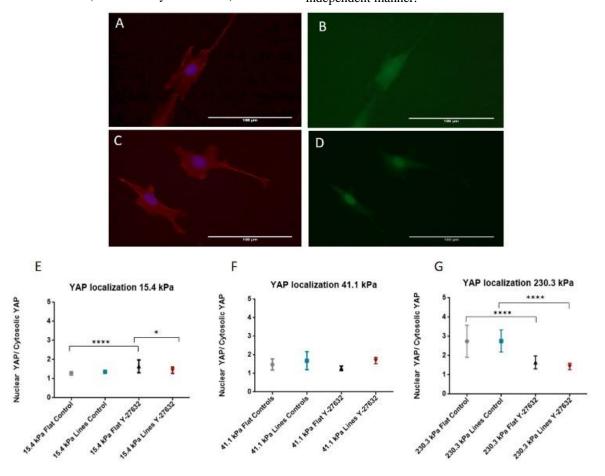

Fig. 7. Representative images of cells with cytosolic YAP (A and B) and nuclear YAP (C and D). A and C show the merge of fluorescent signal of the nuclei (blue) and actin cytoskeleton (red), whereas B and D show the YAP (green). Scale bars 100 μm. Quantification of YAP localization of cells cultured on flat and topographically modified substrates for cells without (controls) and with Y-27632 (20 μM) treatment in soft (E), medium (F) and hard hydrogels (G).

Then, we studied how cell morphology was affected when cell contractility was compromised by inhibiting ROCK I activity with Y-27632. Representative optical microscopy images of cells seeded in flat with Y-27632 are shown in *Fig. 6 A-C* and in topography with Y-27632 in *Fig. 6 D-E*. In relation to the results of the area measurements in presence of Y-27632 (*Fig. 6 G-I*) we can see that when contractility is inhibited, the cellular area of flat conditions is larger than in control samples for all stiffness. Also, comparing the areas of cells on topographically modified substrates both in controls and in the presence of ROCK I inhibitor we can also see an increase in cellular area when contractility is inhibited, and interestingly, this increase is larger on stiffer substrates.

When cell contractility is inhibited, cell elongation and alignment behave in a similar way than control cells. Cells are clearly more elongated on topography than on flat substrates for all stiffness (*Fig. 6 J*), but in this case stiffness increase does not imply rounder cell shapes. Regarding alignment, cells are clearly aligned with topography, whereas on flat substrates they present a random orientation (*Fig. 6 K*).

So, whereas the effects of stiffness on cell morphology (area and circularity increase with stiffness) are compromised when cell contractility is inhibited, the effects of topography (elongation and alignment) are not altered.

C. YAP intracellular localization

Since we observed differences in cell morphology due to the topographical features independently of the substrate stiffness and the cell contractility, we wondered if topography alone could induce YAP translocation to the nucleus. However, YAP localization does not present differences between flat and topography conditions for any stiffness, although it translocates from cytosolic (*Fig. 7 A and B*) to nuclear (*Fig. 7 C and D*) when stiffness increases (*Fig. 7 E-G*), suggesting that the presence of a topographical pattern does not activate YAP translocation. On the contrary, we can see a clear change from nuclear YAP to cytosolic YAP when cell contractility is inhibited for the hardest hydrogels (*Fig. 7 G*). Despite significant differences in the YAP ratios between conditions of the soft hydrogel (*Fig. 7 E*), all values correspond to ratios that indicate a cytosolic localization of YAP. These ratio value are much lower than the ratios than indicate a nuclear localization of YAP. Thus, YAP translocation seems to be contractility dependent and not affected by the presence of topographical cues.

IV. DISCUSSION

We have obtained hydrogels with three different stiffness (15, 41 and 230 kPa) that present very different mechanical cues to the cells seeded on top of them and that are within the physiological range of ECM stiffness [1]. So, the mechanical properties obtained make the fabricated substrates suitable to obtain data that is physiologically relevant and can be indicative of *in vivo* cell response to mechanical cues.

The substrates were characterized with SEM imaging in order to explore the nanoporous nature of the hydrogels. However, we obtained pores at the micrometre range. Although this agrees with previous works [24], we believe that they do not represent the real nature of the hydrogel since we haven't seen them by other means such as AFM (data not shown). Therefore, we suspect that those pores observed in *Fig. 4 B, C and D*, might be an artefact produced during the sample preparation for SEM imaging. This process needs to be optimized to see the real surface, so alternative sample preparation methods such as CO_2 critical point drying can be attempted.

We characterized the effects of the stiffness and topography on cell area, elongation and orientation. We report that cells on flat surfaces increase their spreading area and circularity as stiffness increases, whereas cells on topography spread less than on flat, elongate more than on flat and align with the topographical pattern, regardless of the stiffness. As mentioned above, cell area increases as hydrogel stiffness increments, which is logic if we consider that cell spreading is promoted by higher tensile forces caused by hard substrates, that boost maturation of FA. However, from our experiments it appears that the difference in stiffness between the 15.4 kPa and 41.1 kPa hydrogel is not enough, and we only see this effect when comparing the soft and medium hydrogels to the 230.3 kPa one. Such cell area increase is not seen in the presence of topography. This could be explained by the fact that cells are confined between the lines of the topography and this prevents cell spreading. This confinement would also be more restrictive to cell spreading in harder substrates due to the lines being more rigid than in softer substrates, and this could be the cause of the cellular area being larger in cells seeded in topography in softer hydrogels than in hard ones.

Interestingly, the cellular response to topographical patterns (elongation and alignment) was independent of stiffness, suggesting that the molecular pathways that are involved in the sensing of the substrate compliance could be different that the ones involved in the sensing of the topography. To further explore this hypothesis, contractility (a major actor in mechanical sensing) was reduced by inhibiting ROCK I. Our results showed that, whereas the effects of stiffness in cell morphology (area and circularity increasing with stiffness) were compromised when cell contractility was inhibited, the effects of topography (elongation and alignment) were not altered. When contractility is prevented by inhibition of ROCK I, cell area increases in flat with respect to the topography because cells cannot maintain their shape, as myosin cannot contract. In the case of the topography conditions in presence of Y-27632, this is also true, but the confinement in the topography lines causes lower cell area values. Regarding cell elongation and cell alignment to the topography lines, our findings indicate that inhibition of cell contractility does not have any effect. For both control and ROCK-inhibited conditions, cells are more round and randomly oriented when seeded on flat substrates, whereas they are more elongated and aligned with the lines of the hydrogel when they are seeded on top of the topography. As elongation and alignment are not affected by the loss of cell contractility, it seems that ROCK I is probably not involved in the sensing of topography. On the other hand, as cellular area shows stiffness dependence that is affected when contractility is inhibited, ROCK I is probably involved in the sensing of stiffness.

These results further suggest that the pathways involved in stiffness sensing and topography sensing might be different.

Therefore, we decided to monitor YAP localization as a signature of the activation of the mechanosensing pathways, since YAP is considered as a sensor of mechanical cues, but not of topography ones [14]. YAP localization is clearly nuclear only in the 230.3 kPa hydrogel, and only when cell contractility is present. Once Y-27632 is added, YAP localizes to the cytosol. As said before, YAP localization depends on the substrate stiffness, so if YAP localization is affected when ROCK I is inhibited, this indicates that ROCK I plays a role in stiffness sensing. The results of YAP experiments do not indicate any difference in YAP localization caused by the presence of topography, so, topographical cues do not activate the "sensor of mechanical cues", and this reinforces the idea that these two cues act by different molecular pathways. This idea goes against what has been hypothesized until now, but it is the first time that this topic has been studied using a reliable set-up that allows the total disentanglement of the stiffness and topography cues.

Noteworthy, 41.1 kPa hydrogels are not rigid enough neither to cause YAP localization in the nuclei nor to cause a significant increase in cellular area on flat in comparison to the 15.4 kPa hydrogels, so probably the differences between these two hydrogels is not enough to produce measurable variations in cell behaviour. Furthermore, we have to consider that we are inhibiting ROCK I using Y-27632 and we acknowledge that this inhibitor is working because we see changes in cell area and YAP localization. Even so, it would be interesting in further research to check if correct inhibition of ROCK I is taking place and whether this inhibition is total or partial, for example by measuring the levels of phosphorylated MLC by Western-blot. In addition to this, as inhibition of ROCK is taking place 3 hours after cells are seeded on top of the hydrogels it could be possible that the cause of not seeing changes in cell elongation and alignment is the loss of contractility itself, rather than ROCK I and stiffness not being involved in the determination of these characteristics. For this, further research should study the effect of inhibition of ROCK I by adding the inhibitor at the same time of cell seeding.

In addition, it would be interesting to exploit our experimental set-up to study the implication of microtubules in mechanosensing and topography sensing, as it constitutes the other main element of the cytoskeleton, besides actin. Evidences suggest a complex interplay between the microtubule cytoskeleton, FA maturation and cellular contractile force [25]. Basically, when the microtubule cytoskeleton is disrupted, microtubule-bound GEF-H1 is released and it hyperactivates RhoA and, as a consequence, myosin contractibility is also increased. This increase in contractibility leads to the assembly of stress fibres and FA maturation. However, these studies have not been carried out with topography or with substrates of different stiffness, so it could be interesting to see how these different conditions influence microtubule disruption effects.

Moreover, it would be interesting to carry out the experiment using tumour cells, to better correlate the *in vitro* results to the expected *in vivo* behaviour in tumours that cause the orientation of ECM fibrous proteins.

How physical cues of cell environmental affect cell behaviour, morphology, differentiation and proliferation is currently poorly understood as, historically, biochemical cues and their effects have been the focus of the research. Nevertheless, during the last years, physical and mechanical characteristics of cell surroundings are gaining relevance. This is not surprising, as it has been seen that mechanical cues are involved in morphogenetic processes during the embryonic development [26] and can be the physical basis of some developmental disorders. Also of high importance is the alteration of tensional homeostasis, as perturbation of ECM mechanical properties or its perception by the cells lead to diseases, such as cancer [27], and are involved in tissue degeneration during aging.

V. CONCLUSION

We have shown that our experimental design has allowed us to address the connection between stiffness, topography and cell contractility by disentangling these elements. Results obtained seem to point in the direction of independent pathways for the detection of stiffness and topography, being the latest contractility independent. Our study sheds some light on the role of ROCK I and contractility in the sensing of topography and stiffness. The results obtained indicate that topography and stiffness sensing would be controlled by two different molecular pathways, and that ROCK I and cell contractility would only be involved in the sensing of stiffness. However, some of our results also indicate that cell area is still stiffness dependent when cells are seeded on topography and Y-27632 is added, which goes against our hypothesis that ROCK I needs to be active for stiffness sensing. Further research should be conducted to see if this result is an artefact, or if is truly a tendency that repeats in other experiments. To know more how cells respond to stiffness and topography of their environment is essential for the development of substrates and scaffolds of the adequate characteristics to promote cell survival, differentiation and proliferation for tissue regeneration or for *in vitro* assay platforms for study tissue development, regeneration, model of disease and systems for drugs and therapy testing.

REFERENCES

[1] I. A. Janson and A. J. Putnam, "Extracellular matrix elasticity and topography: material-based cues that affect cell function via conserved mechanisms". *J Biomed Mater Res Part A,* 2015, 103(3):1246-58

[2] J. L. Young, A. W. Holle and J. P.Spatz. "Nanoscale and mechanical properties of the physiological cell-ECM microenviroment". *Exp Cell Res*, 2016, 343(1):3-6

[3] H. Lv, L. Li, M. Sun, Y. Zhang, L. Chen, Y. Rong and Y. Li. "Mechanism of regulation of stem cell differentiation by matrix stiffness" *Stem Cell Res Ther*, 2015, 6(1):103

[4] A. I. Teixeira, G. A. Abrams, P. J. Bertics, C. J. Murphy and P. F. Nealey, "Epithelial contact guidance on well defined micro- and nanostructured substrates". *J Cell Sci,* 2003, 116:1881-1892

[5] P. P. Provenzano, K. W. Eliceiri, J. M. Campbell, D. R. Inman, J. G. White and P. J. Keely. "Collagen reorganization at the tumor-stromal interface facilitiates local invasion". *BMC Medicine*, 2006, 4(1):38

[6] A. Ray, O. Lee, Z. Win, R. M. Edwards, P. W. Alford, D. Kim and P. P. Provenzano. "Anisotropic forces from spatially constrained focal adhesions mediate contact guidance directed cell migration". *Nat Commun*, 2017, 8:14923

[7] B. Geiger, J. P. Spatz and A. D. Bershadsky, "Enviromental sensing through focal adhesions". *Nat Rev Mol Cell Biol,* 2009, 10(1):21-33

[8] Z. Sun, S. S. Guo and R. Fässler. "Integrin-mediated mechanotransduction". *J Cell Biol,*2016, 215 (4):445-456

[9] A. Elosegui-Artola, R. Oria, Y. Chen, A. Kosmalska, C. Pérez-Gonzalez, N. Castro, C. Zhu, X. Trepat and P. Roca-Cusachs. "Mechanical regulation of a molecular clutch defines force transmission and transduction in response to matrix rigidity". *Nat Cell Biol,* 2016, 18(5):540-548

[10] A. C. Canver, O. Ngo, R. L. Urbano, A. M. Clyne. "Endothelial directed collective migration depends on substrate stiffness via localized myosin contractility and cell-matrix interactions". *J Biomech,* 2016, 49(8):1369-1380

[11] M. Amano, M. Nakayama and K. Kaibuchi. "Rho-kinase/ROCK: a key regulatory of the cytoskeleton and cell polarity". *Cytoskeleton,* 2010, 67(9):545-554

[12] C. Ramachandran, R. V. Patil, K. Combrink, N. A. Sharif and S. P. Srinivas. "Rho-Rho kinase pathway in the actomyosin contraction and cell-matrix adhesion in immortalized human trabecular meshwork cell". *Mol Vis*, 2011,17:1877-1890

[13] S. Dupont, L. Morsut, M. Aragona, E. Enzo, S. Giulitti, M. Cordenonsi, F. Zanconato, J. Le Digabel, M. Forcato, S. Bicciato, N. Elvassore and S. Piccolo. "Role of YAP/TAZ in mechanotransduction*"*. *Nature*, 2011,474(7350):179-183

[14] G. Halder, S. Dupont and S. Piccolo, "Transduction of mechanical and cytoskeletal cues by YAP and TAZ". *Nat Rev Mol Cell Biol*, 2012, 13(9):591-600

[15] A. Calzado-Martín, A. Méndez-Vilas, M. Multigner, L. Saldaña, J. L. González-Carrasco, M. L. González-Martín and N. Vilaboa. "On the role of RhoA/ROCK signalling in contact guidance of bone-forming cells on anisotropic Ti6Al4V surfaces". *Acta Biomater*, 2011, 7(4):1890-901

[16] A. M. Raijnieck, L. E. Foubister and C. D. McCaig. "Prioritising guidance cues: directional migration induced by substratum contours and electrical gradients in controlled by a rho/cdc42 switch". *Dev Biol*, 2007, 312(1):448-60

[17] A. C. Saito, T. S. Matsui, T. Ohishi, M. Sato and S. Dequchi. "Contact guidance of smooth muscle cells is associated with tension-mediated adhesion maturation". *Exp Cell Res*, 2014, 327(1):1-11

[18] D. Franco, M. Klingauf, M. Bednarzik, M. Cecchini, V. Kurtcuoglu, J. Gobrecht, D. Poulikakos and A. Ferran. "Control of initial endothelial spreading by topographic activation of focal adhesion kinase". *Soft Matter*, 2011, 7:7313

[19] S. V. Plotnikov, B. Sabass, U. S. Schwarz and C. M. Waterman, "High-resolution traction force microscopy". *Methods Cell Biol*, 2014, 123: 367-394

[20] T. Takigawa, Y. Morino, K. Urayama and T. Masuda. "Poisson's ratio of polyacrylamide (PAAm) gels. *Polym Gels Netw,* 1996, 4(1):1-5

[21] J. Alcaraz, L. Buscemi, M. Grabulosa, X. Trepat, B. Fabry, R. Farré and D. Navajas. "Microrheology of human lung epithelial cells measured by atomic force microscopy". *Biophys J*, 2003, 84(3):2071-2079

[22] R. S. Fischer, K. A. Myers, M. L. Gardel and C. M. Waterman. "Stiffness-controlled three-dimensional extracellular matrices for high resolution imaging of cell behaviour". *Nat. Protoc*, 2012,7(11):2056-2066

[23] J. Schindelin, I. Arganda-Carreras, E. Frise, V. Kaynig, M. Longair, T. Pietzsch, S. Preibisch, C. Rueden, S. Saalfeld, B. Schmid, J. Y. Tinevez, D. J. White, V. Hartenstein, K. Eliceiri, P. Tomancak and A. Cardona. "Fiji: an open-source platform for biological-image analysis". *Nat Methods*, 2012, 9(7):676-682

[24] J. H. Wen, L. G. Vincent, A. Fuhrmann, Y. S. Choi, K. C. Hribar, H. Taylor-Weiner, S. Chen and A. J. Engler. "Interplay of matrix stiffness and protein tethering in stem cell differentiation". *Nat Mater*, 2014, 13(10):979-987

[25] H. J. Ng. Daniel, J. D. Humphries, A. Bryon, A. Millon-Frémillon and M. J. Humphries. "Microtubule-dependent modulation of adhesion complex composition". *PLoS ONE,* 2014, 9(12):e115213

[26] T. Mammoto and D. E. Ingber. "Mechanical control of tissue and organ development". *Development*, 2010, 137(9):1407-1420.

[27] R. Malik, P. I. Lelkes and E. Cukierman. "Biomechanical and biochemical remodelling of stromal extracellular matrix in cancer". *Trends Biotechnol*, 2015, 33(4):230-236